Porphyrin Dyes with High Injection and Low Recombination for Highly Efficient Mesoscopic Dye-Sensitized Solar Cells

Eva M. Barea,*,[†] Victoria Gónzalez-Pedro,[†] Teresa Ripollés-Sanchis,[†] Hui-Ping Wu,[‡] Lu-Lin Li,[‡] Chen-Yu Yeh,[§] Eric Wei-Guang Diau,*,[‡] and Juan Bisquert[†]

[†]Photovoltaic and Optoelectronic Devices Group, Physics Department, Universitat Jaume I, 12071 Castelló, Spain

[‡]Department of Applied Chemistry and Institute of Molecular Science, National Chiao Tung University, Hsinchu, 300, Taiwan

[§]Department of Chemistry, National Chung Hsing University, Taichung 402, Taiwan

Ⓢ *Supporting Information*

ABSTRACT: The photovoltaic performance and charge recombination character-istics of porphyrin-based dye-sensitized solar cell (DSC) devices have been investigated using the impedance spectroscopy (IS) technique. The IS results provide key information related to the device performance for a highly efficient porphyrin dye (YD2), a reference porphyrin dye (YD0), and a commercial ruthenium dye (N719). The DSC devices constructed using YD2 and N719 dyes reach similar internal power conversion efficiencies (7.41% vs 7.54%) due to the higher injection of the YD2 dye that is compromised by a lower photovoltage. In addition, both YD2 and N719 dyes exhibit the same charge-transfer resistance, indicating that the recombination rates of both dyes are very similar. The diarylamino group plays a key role to repel the triiodide ions from the titania surface so that the charge recombination of YD2 is less significant compared with that of YD0.
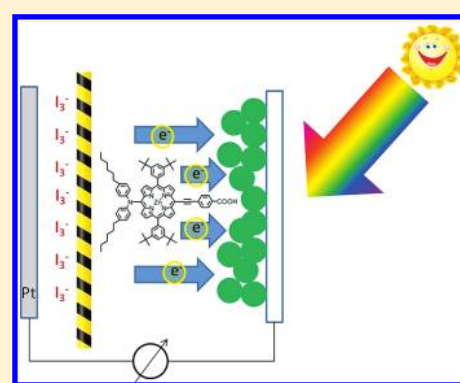
INTRODUCTION

Nanocrystalline semiconductor-based dye-sensitized solar cells (DSCs) have attracted significant attention as low-cost alternatives to conventional solid-state photovoltaic devices.[1] The most successful dye sensitizers employed so far in these cells are polypyridyl-type ruthenium complexes[2,3] yielding over-all AM 1.5 solar-to-electric power conversion efficiencies (PCEs) of up to 11.7%.[4] However, the high cost of ruthenium, the necessity of purification treatments, and the low molar absorp-tion coefficients pose difficulties for commercialization of large DSC modules, hence the increase in interest in research on organic dyes.[5−7] The advantages of the organic dyes include a small cost of production, tunable electrochemical and photo-physical properties, feasible modification of their molecular structures, and lack of pollution and resource limitation.

A large number of organic dyes, such as polyene-triphenyl-amine,[5,8,9] coumarin,[10,11] phthalocyanine,[12−15] and indoline,[16] have been synthesized for DSCs, obtaining efficiencies of 5−9%.[17] Usually, most of them feature a donor−π conjugated unit−acceptor (D−π−A) structure.[18] Bearing such an approach in mind, the DSC device made of a push−pull porphyrin dye (named YD2; its molecular structure is shown in Figure 1) has reached the benchmark PCE (11%)[19] comparable to that of a Ru-based DSC.

The interest of using porphyrins started from their important role in the efficient energy and electron transfer in the light-harvesting antenna of biological systems. On the basis of this idea, several self-assembled porphyrins have been designed and widely used in photovoltaic devices.[20−22] Porphyrins are mol-ecules that contain a heterocyclic macrocycle with a π-aromatic core, showing an intense Soret band at 400−450 nm and moderate Q bands at 500−650 nm.[15] Compared to the ruthenium complexes, these narrow bands limit the light-harvesting properties in porphyrin-based DSCs. However, it has been demonstrated that elongation of the π conjugation and loss of symmetry causes broadening and a red shift of the absorption bands in porphyrins.[15,23−25] Different substituents to the porphyrin ring have been studied in meso or β positions that favor the injection. One design strategy for increasing the light absorption is to lock the meso-bridge into the plane of the macrocycle in order to improve the π conjugation between the porphyrin and the bridge[13] directly linked to the anchoring group, as close as possible to the chromophore to maximize coupling between the porphyrin and the TiO$_2$.[14] The incor-poration of a push−pull moiety in the meso position of porphyrin, opposite to the anchoring group, increases the efficiency due to a good compromise between suppression of dye aggregation, extension of the π-conjugated system, and enhancement of the charge-transfer directionality in the excited state.[14]
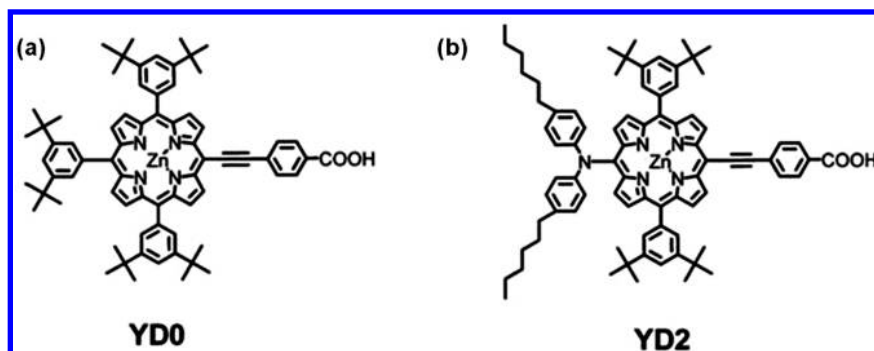
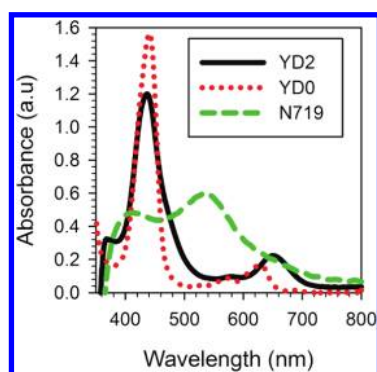**Figure 1.** Dye structure for (a) YD0 and (b) YD2 porphyrin dyes.

Figure 2. UV−vis spectra for YD2 and YD0 dyes absorbed on transparent titania film.

Additionally, they present good photostability and high light-harvesting capabilities that favor applications in low-cost thin-film DSCs. Despite adequate characteristics that porphyrins present to be used as sensitizers and the highest efficiency reported recently,[19] there are many functional factors that are still not clear. For example, why can porphyrin dyes, especially YD2, achieve such a high performance close to that of a Ru commercial dye? Besides the dye structure and the related photophysical properties, what other key parameters in a DSC influence strongly the overall power conversion efficiency?

To address these questions, we have carried out impedance spectroscopy (IS) and photoelectrochemical measurements for the highly efficient porphyrin dye YD2, a reference porphyrin dye (YD0), and a commercial ruthenium dye (N719) that provide information on the role of the sensitizer in the device performance.[12,26,27] The analyzed results corresponding to the electron transport and charge recombination characteristics are well correlated to the overall power conversion efficiencies of the devices.

■ EXPERIMENTAL SECTION

Synthesis and Characterization of YD0 and YD2. The synthesis, photophysical and electrochemical properties, and photovoltaic characteristic of the two zinc porphyrin dyes, YD0 and YD2, used in this study have been reported previously by Lu et al.[28] As shown in Figure 1, YD2 consists of a diarylamino group with two hexyl chains attached to the porphyrin ring acting as an electron donor, π-conjugated phenylethynyl group as a bridge, and the carboxylic acid moiety as an acceptor. The porphyrin chromophore itself constitutes the π bridge as a light-harvesting

center in this particular D−π−A structure.[28,29] Without the diarylamino substituent, YD0 serves as a reference dye to test the effect of the electron donor.

The UV−vis absorption spectra of YD0 and YD2 sensitized on TiO$_2$ films are shown in Figure 2 for comparison. The absorbance of YD2 is higher and substantially shifted toward the longer wavelength region due to the effective π conjugation of the diarylamino donor with respect to the porphyrin macro-cycle. The absorption spectrum of the N719 dye presents the normal shape. All the UV−vis absorption spectra of the dye/TiO$_2$ films were taken under the same conditions (on 2 μm transparent titania film for 2 h). To determine the dye-loading amount of the YD0 and YD2 on TiO$_2$ films, we desorbed the dye in tetrabutylammonium hydroxide solution (0.1 M in ethanol) and recorded the absorption spectrum of the solution (not shown).[28]

DSC Fabrication and Characterization. The DSC devices were fabricated according to a sandwich-type structure. The working electrodes contain the TiO$_2$ nanocrystalline pastes purchased from Dyesol (18NR-T). The TiO$_2$ layers were deposited on transparent conducting oxide (TCO) glass (Pilkington TEC15, ∼15Ω/sq resistance) using the doctor blade technique. The resulting photoelectrodes of 7 μm thickness were sintered at 450 °C and then immersed in 0.04 M TiCl$_4$ solution for 30 min at 70 °C, followed by calcination at 570 °C for 30 min to obtain a good electrical contact between the nanoparticles. When the temperature decreased until 40 °C, all the electrodes were immersed into the dye solutions overnight. The YD0 dye (0.2 mM) was coadsorbed with chenodeoxycholic acid (CDCA) in anhydrous ethanol ([dye]/[CDCA] = 1/2). The YD2 dye (0.2 mM) solution was prepared in anhydrous ethanol without adding CDCA according to conditions reported previously.[28] The N719 dye (0.3 mM) solution was prepared in acetonitrile/*tert*-butanol (v/v = 1:1) as a reference (Ru dye reference). After the adsorption of the dye on TiO$_2$ films, the working electrodes were rinsed with the same solvent used for dye solution. The DSC devices were assembled with a counter electrode (thermally platinized TCO) using a thermoplastic frame (Surlyn, 25 μm thick). Redox electrolyte (lithium iodide (LiI, 0.1 M), diiodine (I$_2$, 0.05 M), PMII (0.6 M), and TBP (0.5 M) in a mixture of acetonitrile and methoxypropionitrile (v/v = 1:1)) was introduced though a hole drilled in the counter electrode that was sealed afterward.

Prepared solar cells (0.3 cm^2 size, masking solar cell to 0.25 cm^2) were characterized by current density−voltage (*j*−V) characteristics and IS. Photocurrents and voltages were measured using a solar simulator equipped with a 1000 W
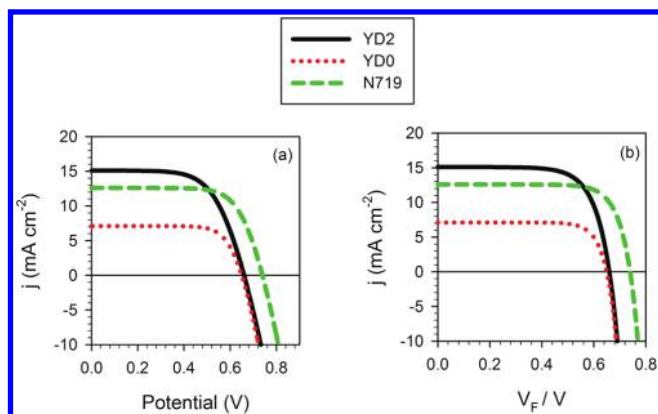
10899

dx.doi.org/10.1021/jp2018378 |*J. Phys. Chem. C* 2011, 115, 10898−10902

Figure 3. $j-V$ curves for DSCs prepared with YD2, YD0, and N719 dyes, with transparent titanium nanoparticles 7 μm thick (a) and $j-V$ curves that have been corrected for the series resistance (b).
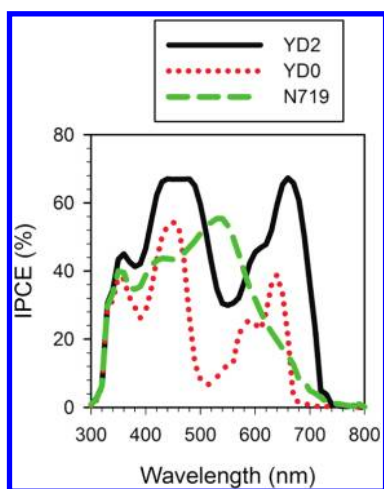

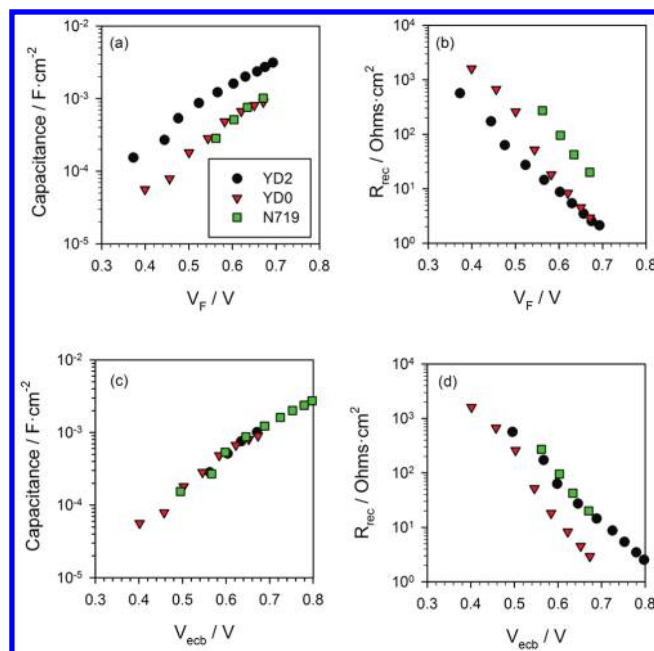**Figure 4.** IPCE for DSCs prepared with YD2, YD0, and N719.

Figure 5. (a) Capacitance and (b) recombination resistance, with respect to the Fermi level voltage (removing the effect of series resistance). (c) Capacitance and (d) recombination resistance replotted with respect to the equivalent common conduction band voltage so that the distance between the Fermi level and the conduction band is the same in all cases.

Table 1. Photovoltaic Performances of the DSCs Sensitized with YD2, YD0 and N719, and Parameters Obtained by Combination of Both j-V and Impedance Data[a]

	sample		
	YD2	YD0	N719
V_{oc} (V)	0.66	0.65	0.74
j_{sc} (mA/cm^2)	15.4	6.92	12.6
FF	0.62	0.73	0.70
efficiency (%)	6.36	3.29	6.54
β	0.47	0.73	0.70
j_0 (mA/cm^2)	7.75×10^{-5}	6.09×10^{-8}	2.09×10^{-8}
j_{0k} (mA/cm^2)	54	1406	213
α	0.29	0.30	0.24
$\triangle E_c$ vs ref (mV)	-123	-32.0	ref
R_{series} (Ω)	19.5	19.4	17.9
internal FF	0.73	0.81	0.81
internal efficiency (%)	7.41	3.58	7.54

[a] Values of V_{oc}, FF, j_{sc}, and efficiency are obtained at steady-state measurement under 100 mW cm^{-2} light intensity and AM 1.5 global radiation. β is a recombination parameter, j_0 is the dark current, j_{0k} is the charge-transfer constant, α is the exponential states distribution in the band gap of titania, $\triangle E_c$ vs ref is the potential shift to compare all the cells at the same capacitance, R_{series} is the series resistance (given a constant value to simplify the analysis), and internal FF and efficiency are calculated without effect of series resistance.

ozone-free xenon lamp and a AM 1.5G filter (Oriel), and the light intensity was adjusted according to an NREL-calibrated Si solar cell with a KG-5 filter to 1 sun intensity (100 mW cm^{-2}). IS measurements were carried out under an irradiation of 1 sun (AM 1.5 conditions), and different bias potentials that ranged from zero to open-circuit voltage and frequencies between 1 MHz and 0.1 Hz.

■ RESULTS AND DISCUSSION

The DSC devices made of sensitizers YD0, YD2, and N719 were characterized by $j-V$ curves (Figure 3a), incident photon-to-current conversion efficiency (IPCE) (Figure 4), and IS (Figure 5); the resulting photovoltaic and impedance parameters are summarized in Table 1. Note that the N719 dye presents the highest open-circuit voltage (V_{oc}) in comparison with those of both porphyrin dyes (YD0 and YD2). It was reported that this phenomenon could be related to the rapid recombination of electrons on the TiO$_2$ surface with the I$_3^-$ ions in the redox electrolyte, which strongly decreases the V_{oc} values for the organic dyes.[30] Nevertheless, YD2 presents the largest photocurrent density, 15.4 mA cm^{-2}, even higher than that of N719 (12.6 mA cm^{-2}).

The lower photocurrent observed for the YD0 dye is related to the amounts of dye loading, which are 104 and 159 nmol cm^{-2} for YD0 and YD2, respectively. The large dye-loading amount of

YD2 might be attributed to the following two points. First, the alkyl group attached to the donor side of YD2 should improve the solubility of the dye in solution. Second, YD0 is coadsorbed with CDCA in a 2/1 ratio on TiO_2 films, whereas for YD2, uptake of the CDCA was absent.[28] Because the capacity of dye loading is related to the capability of photon capture, the higher dye loading provides the better light-harvesting efficiency (LHE) and hence increases the short-circuit current (j_{sc}) of the photovoltaic device.

The lower value of V_{oc} for YD2 is compensated by the higher j_{sc} value, giving an overall conversion efficiency of 6.36%, which is close to that of a commercial N179 dye (6.54%). Also, the peak of IPCE for YD2 (70%) is higher than that of N719 and that of YD0 (56% for both dyes). There is a large gap between the Soret and the Q bands for YD0 and YD2 because the working electrodes consist of only transparent TiO_2 films in the absence of a scattering layer.

To clarify the mechanism governing the performance of the device, IS measurements were performed on the DSCs at different bias potentials under 1 sun irradiation. These measurements were analyzed using the impedance model developed by Bisquert and co-workers,[31,32] allowing us to isolate the recombination resistance from other resistive contributions in the cell. The aim of IS measurements here is to identify the variations in the devices concerning an upward shift of the conduction band of TiO_2, E_c, or a decrease of the rate of recombination, because it has been observed that organic dyes exert a strong influence on the rate of charge transfer.[33] Details about these methods and the interpretation of IS results in connection to the performance of DSCs are provided in recent papers.[12,26,27,34]

Figure S1a,b in the Supporting Information shows the measured capacitance, C_μ, and recombination resistance, R_{rec}, as a function of the potential for the different cells. C_μ gives quantitative information about the position of the conduction band, while R_{rec} is directly related to the recombination flux through eq 1.[27]

$$R_{rec} = \frac{1}{A}\left(\frac{\partial j_{rec}}{\partial V}\right)^{-1} \qquad (1)$$

Here, j_{rec} is the recombination current and A is the cell area. IS enables extracting the voltage drop in the sensitized electrode, V_F, at each applied potential, V_{app}, by subtracting the effect of the series resistance on both R_{rec} and C_μ as follows: $V_F = V_{app} - V_s - V_{ce}$, where V_s and V_{ce} are potential drops at the series resistance and at the counter electrode, respectively. V_F is proportional to the rise of the Fermi level of electrons in TiO_2, $V_F = (E_{Fn} - E_{F0})/q$, where q is the positive elementary charge and E_{Fn} and E_{F0} are the electron quasi-Fermi level and the electron Fermi level at the equilibrium, respectively (Figure 5a,b). To analyze the recombination resistance, R_{rec}, on the basis of a similar number of electrons (i.e., the same distance between the electron Fermi level, E_{Fn}, and conduction band (CB) of TiO_2, E_{CB}), the shift of the CB has been corrected in the potentials of Figure 5c,d, where the voltage scale is V_{ecb} (equivalent common conduction band voltage).[26,27] The criterion for the modified scale is that the chemical capacitances of the analyzed samples overlap (Figure 5c) because the chemical capacitance is directly related to the difference $E_{CB} - E_{Fn}$, by the relation, $C_\mu \propto \exp[-(E_{CB} - E_{Fn})/(k_B T)]$. The same shift applied to the chemical capacitance has been applied to the R_{rec} shown in Figure 5d. All the graphs from Figure 5 and the

parameters shown in the lower part of Table 1 have been implemented in specific software for data treatment.[26]

From the analysis of C_μ (Figure 5a), we can straightforwardly identify the downward shift of the conduction band edge of titania in the case of the DSC fabricated with the YD2 dye. As is well-known,[26] the lower position of the conduction band facilitates the electron injection from the dye to TiO_2 and tends to increase the photocurrent. The downward shift of E_{CB} decreases the energy difference between E_{CB} and the I^-/I_3^- redox potential of the electrolyte, resulting in a lower V_{oc} (see Table 1). Figure 5c,d shows the logarithmic plots of C_μ and R_{rec}, respectively, for three DSC devices as a function of equivalent common conduction band voltage (the reference dye is N719, and the shifts in the potential of YD0 and YD2 are shown in Table 1, $\triangle E_c$ vs ref). It is clearly observed that the R_{rec} values of YD0 are smaller than those of YD2 and N719 under the same E_{CB} level, indicating that charge recombination is more significant for the former than the latter. This explains the lower V_{oc} and the lower injection for YD0.[34] As shown in Table 1, it is observed that YD0 presents, in a good correlation with Figure 5d, the highest charge-transfer constant value ($j_{0k} = 1406$ mA cm^{-2}).

In the case of YD2 and N719, both of them show almost the same recombination resistance (Figure 5d), so the higher injection of the YD2 dye is explained due to a downward displacement of the conduction band of the mesoporous titania (Figure 5a). As a result, the YD2 device compensates its lower V_{oc} with the higher injection to give an overall conversion efficiency comparable to that of the N719 device. To compare between YD2 and N719, the differences in the charge-transfer parameter, j_{0k} (54 vs 213 mA cm^{-2}), and in the recombination parameter, β (0.47 vs 0.70), are attributed to the shift of the conduction bands of the titania films, though the R_{rec} values are very similar when they were measured at the same V_{ecb}.

Removing the contributions of V_s and V_{ce} point to point, we can re-evaluate the photovoltaic characteristics of the DSC devices. The reanalyzed $j-V$ curves are shown in Figure 3b, and the corrected (internal) FFs and efficiencies are listed in Table 1. According to this approach, the FF values are enhanced with the same values of V_{oc} and j_{sc} determined experimentally. This analysis thus provides a measure of the performance of the materials that form the photoelectrode for DSCs. The results show that YD2 and N719 have essentially the same performance in terms of conversion efficiency at 1 sun (7.41% vs 7.54%). The lower performance of YD2 than N719 in the experimental data is because YD2 has a large current, being that the effect of the series resistance is more important in the FF (0.73 for YD2 and 0.81 for N719). This trend is well correlated with the calculated parameters (R_{series}) obtained with the simulation (Table 1).

The analysis of IS data in the measured solar cells indicates that the main factor affecting the charge recombination and the overall performance in the DSC is the functional group of the dye. The electron-donor group in YD2 has the feature to extend the absorption spectrum to the near-infrared region of the solar spectrum, to increase the electron injection rate by the push−pull effect, and to keep the I_3^- away from the titania surface so as to decrease the charge recombination rate like the effect of the thiocyanate substituent groups in the N719 dye.[35,36] In the case of YD0, which does not involve the diarylamino donor group, the recombination resistance is smaller and j_{0k} is higher, and this effect has been observed

10901

dx.doi.org/10.1021/jp2018378 |*J. Phys. Chem. C* 2011, 115, 10898–10902

in the reduced internal PCE (3.58%). For the YD2 dye involving an electron-donor group with two hexyl chains, charge recombination becomes substantially inhibited and this leads to YD2 to operate as an efficient sensitizer (7.41%) similar to N719 (7.54%).

■ CONCLUSIONS

The results presented in this study highlight the recombination as the main factor limiting the overall efficiency in the porphyrin-based DSCs. The recombination resistance of the DSCs is strongly influenced by the dye structure. We have shown that the porphyrin dye YD2 exhibits the same cell performance as a ruthenium dye N719 because both dyes feature the same charge-transfer resistance. The diarylamino donor group in the YD2 dye plays the same role in cell performance as the thiocyanate substituent in the N719 dye. For YD0 without an electron-donating group, charge recombination becomes more significant so as to reduce its cell performance in comparison with those of YD2 and N719 dyes.

■ ASSOCIATED CONTENT

S **Supporting Information.** Figure showing the recombination resistance and capacitance, obtained from IS, of the solar cells with YD0, YD2, and N719 as sensitizers. This material is available free of charge via the Internet at http://pubs.acs.org.

■ AUTHOR INFORMATION

Corresponding Author
*E-mail: barea@fca.uji.es (E.M.B.), diau@mail.nctu.edu.tw (E.W.-G.D.).

■ ACKNOWLEDGMENT

■ REFERENCES

(1) O'Regan, B.; Grätzel, M. *Nature* **1991**, *353*, 737.

(2) Kay, A.; Nazeeruddin, M. K.; Rodicio, I.; Humphry-Baker, R.; Muller, E.; Linska, P.; Vlachopoulus, N.; Grätzel, M. *J. Am. Chem. Soc.* **1993**, *115*, 6382.

(3) Pechy, P.; Rotzinger, F. P.; Nazeeruddin, M. K.; Kohle, O.; Zakeeruddin, S. M.; Humphry-Baker, R.; Grätzel, M. *J. Chem. Soc., Chem. Commun.* **1995**, 65.

(4) Yu, Q.; Wang, Y.; Yi, Z.; Zu, N.; Zhang, J.; Zhang, M.; Wang, P. *ACS Nano* **2010**, *4*, 6032.

(5) Kim, S.; Lee, J. K.; Kang, S. O.; Ko, J.; Yum, J. H.; Fantacci, S.; De Angelis, F.; Di Censo, D.; Nazeeruddin, M. K.; Grätzel, M. *J. Am. Chem. Soc.* **2006**, *128*, 16701.

(6) Liang, M.; Xu, W.; Cai, F.; Chen, P.; Peng, B.; Chen, J.; Li, Z. *J. Phys. Chem. C* **2007**, *111*, 4465.

(7) Hagberg, D. P.; Marinado, T.; Karlsson, K. M.; Nonomura, K.; Qin, P.; Boschloo, G.; Brinck, T.; Hagfeldt, A.; Sun, L. *J. Org. Chem.* **2007**, *72*, 9550.

(8) Edvinsson, T.; Hagberg, D. P.; Marinado, T.; Boschloo, G.; Hagfeldt, A.; Sun, L. *Chem. Commun.* **2006**, *21*, 2245.

(9) Hagberg, D. P.; Yum, J. H.; Lee, H.; De Angelis, F.; Marinado, T.; Karlsson, K. M.; Humphry-Baker, R.; Sun, L.; Hagfeldt, A.; Gratzel, M.; Nazeeruddin, M. K. *J. Am. Chem. Soc.* **2008**, *130*, 6259.

(10) Hara, K.; Sato, T.; Katoh, R.; Furube, A.; Yoshihara, T.; Murai, M.; Kurashige, M.; Ito, S.; Shinpo, A.; Suga, S.; Arakawa, H. *Adv. Funct. Mater.* **2005**, *15*, 246.

(11) Hara, K.; Sato, T.; Katoh, R.; Furube, A.; Ohga, Y.; Shinpo, A.; Suga, S.; Sayama, K.; Sugihara, H.; Arakawa, H. *J. Phys. Chem. B* **2003**, *107*, 597.

(12) Barea, E.; Ortiz, J.; Payá, F. J.; Fernández-Lázaro, F.; Fabregat Santiago, F.; Sastre-Santos, A.; Bisquert, J. *Energy Environ. Sci.* **2010**, *3*, 1985.

(13) Waltera, M. G.; Rudineb, A. B.; Wamser, C. C. *J. Porphyrins Phthalocyanines* **2010**, *14*, 759.

(14) Martínez-Díaz, M. V.; de la Torrea, G.; Torres, T. *Chem. Commun.* **2010**, *46*, 7090.

(15) Imahori, H.; Umeyama, T.; Ito, S. *Acc. Chem. Res.* **2009**, *42*, 1809.

(16) Daibin, K.; Satoshi, U.; Robin, H. B.; Shaik, M. Z.; Gratzel, M. *Angew. Chem., Int. Ed.* **2008**, *47*, 1923.

(17) Ho Lee, J.; Hwang, S.; Park, C.; Lee, H.; Kim, C.; Park, C.; Lee, M.; Lee, W.; Park, J.; Kim, K.; Park, N. G.; Kim, C. *Chem. Commun.* **2007**, 4887.

(18) Mishra, A.; Fisher, M. K. R.; Bäuerle, P. *Angew. Chem., Int. Ed.* **2009**, *48*, 2474.

(19) Bessho, T.; Zakeeruddin, S. M.; Yeh, C.-Y.; Wei-Guang Diau, E.; Gratzel, M. *Angew. Chem., Int. Ed.* **2010**, *49*, 6646.

(20) Campbell, W. M.; Jolley, K. W.; Wagner, P.; Wagner, K.; Walsh, P. J.; Gordon, K.-C.; Schmidt-Mende, L.; Nazeeruddin, M. K.; Wang, Q.; Gratzel, M.; Officer, D. L. *J. Phys. Chem. C* **2007**, *111*, 11760.

(21) Eu, S.; Hayashi, S.; Umeyama, T.; Matano, Y.; Araki, Y.; Imahori, H. *J. Phys. Chem. C* **2008**, *112*, 4396.

(22) Cid, J. J.; Yum, J.-H.; Jang, S.-R.; Nazeeruddin, M. K.; Martinez-Ferrero, E.; Palomares, E.; Ko, J.; Gratzel, M.; Torres, T. *Angew. Chem., Int. Ed.* **2007**, *46*, 8358.

(23) Lee, C. Y.; Hupp, J. T. *Langmuir* **2010**, *26*, 3760.

(24) Wu, S.-L.; Lu, H.-P.; Yu, H.-T.; Chuang, S.-H.; Chiu, C.-L.; Lee, C.-W.; Diau, E.; Yeh, C.-Y. *Energy Environ. Sci.* **2010**, *3*, 949.

(25) Barea, E.; Caballero, R.; López-Arroyo, L.; Guerrero, A.; De la Cruz, P.; Langa, F.; Bisquert, J. *ChemPhysChem* **2011**, *12*, 961.

(26) Barea, E.; Zafer, C.; Gultekin, B.; Aydin, B.; Koyuncu, S.; Icli, S.; Fabregat Santiago, F.; Bisquert, J. *J. Phys. Chem. C* **2010**, *114*, 19840; see also www.istest.eu.

(27) Fabregat-Santiago, F.; Garcia-Belmonte, G.; Mora-Seró, I.; Bisquert, J. *Phys. Chem. Chem. Phys.* **2011**, *13*, 9083−9118.

(28) Lu, H.-P.; Tsai, C.-Y.; Yen, W.-N.; Hsieh, C.-P.; Lee, C.-W.; Yeh, C.-Y.; Diau, E. W.-G. *J. Phys. Chem. C* **2009**, *113*, 20990.

(29) Hsieh, C.-P.; Lu, H.-P.; Chiu, C.-L.; Lee, C.-W.; Chuang, S.-H.; Mai, C.-L.; Yen, W.-N.; Hsu, S.-J.; Diau, E. W.-G.; Yeh, C.-Y. *J. Mater. Chem.* **2010**, *20*, 1127.

(30) Li, R.; Lv, X.; Shi, D.; Zhou, D.; Cheng, Y.; Zhang, G.; Wang, P. *J. Phys. Chem. C* **2009**, *113*, 7469.

(31) Bisquert, J. *J. Phys. Chem. B* **2002**, *106*, 325.

(32) Fabregat-Santiago, F.; Bisquert, J.; Palomares, E.; Otero, L.; Kuang, D.; Zakeeruddin, S.; Gratzel, M. *J. Phys. Chem. C* **2007**, *111*, 6550.

(33) O'Regan, B.; Durrant, J. R. *Acc. Chem. Res.* **2009**, *42*, 1799.

(34) Barea, E. M.; Caballero, R.; Fabregat-Santiago, F.; de la Cruz, P.; Langa, F.; Bisquert, J. *ChemPhysChem* **2010**, *11*, 245.

(35) Morandeira, A.; Lopez-Duarte, I.; O'Regan, B.; Martinez-Diaz, M. V.; Forneli, A.; Palomares, E.; Torres, T.; Durrant, J. R. *J. Mater. Chem.* **2009**, *19*, 5016.

(36) Mozer, A. J.; Griffith, M. J.; Tsekouras, G.; Wagner, P.; Wallace, G. G.; Mori, S.; Sunahara, K.; Miyashita, M.; Earles, J. C.; Gordon, K. C.; Du, L.; Katoh, R.; Furube, A.; Officer, D. L. *J. Am. Chem. Soc.* **2009**, *131*, 15621.